

Numerical approximations of the Ginzburg–Landau models for superconductivity

Qiang Du^{a)}

*Department of Mathematics, Pennsylvania State University,
University Park, Pennsylvania 16802*

(Received 16 May 2005; accepted 17 May 2005; published online 29 September 2005)

In this paper, we review various methods for the numerical approximations of the Ginzburg–Landau models of superconductivity. Particular attention is given to the different treatment of gauge invariance in both the finite element, finite difference, and finite volume settings. Representative theoretical results, typical numerical simulations, and computational challenges are presented. Generalizations to other relevant models are also discussed. © 2005 American Institute of Physics.
[DOI: [10.1063/1.2012127](https://doi.org/10.1063/1.2012127)]

I. INTRODUCTION

The macroscopic model of Ginzburg and Landau^{43,91} has been widely used to study both low-temperature and high-temperature superconductors. Due to its highly nonlinear nature, the complex energy landscape and the exotic dynamic responses of its solution to external conditions, its numerical simulations have become valuable tools in order to better understand the properties of the Ginzburg–Landau (GL) models and to provide further theoretical insight into the intriguing superconductivity phenomena.

The development of approximation methods of the Ginzburg–Landau model goes back to the 1950s shortly after the inception of the model.⁵⁸ Particularly notable works include the seminal paper by Abrikosov² on the vortex state in type-II superconductors based on the linearization of GL equations near the upper critical field. The systematic studies of the GL models from the numerical analysis point of view, to our knowledge, have not been seriously developed until the publication of Ref. 43. In Ref. 43, both rigorous mathematical theory on the well-posedness of the equilibrium GL models and their physical background were presented, along with the systematic development of finite element approximation methods. The work in Ref. 43 was partly motivated by Refs. 3 and 29 of casting the equilibrium models into a variational framework. Extensions to the dynamic models, i.e., the time-dependent Ginzburg–Landau (TDGL) equations were subsequently made.^{32,31} Since then, many other works have appeared in the literature, including the development of different types of numerical approximations of Ginzburg–Landau-type models, their rigorous theoretical analysis as well as extensive simulations. By now, almost all aspects of modern numerical analysis have been utilized by people working on the numerical solutions of the GL models, ranging from the design and applications of various discretization methods and fast algorithms, domain decomposition and parallelization techniques, and adaptive computation strategies. In this paper, we briefly review some of the works concerning the numerical approximations of the Ginzburg–Landau models. In terms of spatial discretization methods, we consider, in particular, the finite difference methods, finite element methods and finite volume methods. We also discuss various time-stepping schemes for time dependent models. As there have been a large amount of works on the numerical simulations of the GL models in the last few decades, we make no attempt to provide a comprehensive survey on all existing works on the subject due to limited

^{a)}Electronic mail: qdu@math.psu.edu

space. In particular, our review of the vast physics literature is very much limited to those that have also received much attention in the numerical analysis community or have been examined more rigorously in the mathematics literature.

The rest of the paper is organized as follows: in Sec. II, we briefly recall the GL models and their basic features. In Sec. III, various numerical schemes are discussed, and in Sec. IV, some sample simulation results are presented and some concluding remarks are given in Sec. V.

We end the introduction by stating that much of the research works discussed in the paper are aimed at the development and refinement of mesoscale and macroscale models for superconductivity so to enlarge the range of physical problems for which such models are valid; the analysis of these models in order to gain further understanding of their properties and of their solutions, and for the most part of the paper, the development, analysis, and the implementation of algorithms for the numerical simulation of the superconductivity models.

II. GINZBURG–LANDAU MODELS

Let $\Omega \subset R^d$ ($d=2, 3$) be the region occupied by the superconducting sample. The primary variables used in the GL models are the complex scalar-valued *order parameter* ψ , the real vector-valued *magnetic potential* \mathbf{A} , and the real scalar-valued electric potential $\bar{\Phi}$. In a non-dimensional form, these variables are related to the physical variables by

density of superconducting charge carriers, $|\psi|^2$,

induced magnetic field, $\text{curl } \mathbf{A}$,

current, $\mathbf{J} = \text{curl } \text{curl } \mathbf{A}$,

electric field, $\frac{\partial}{\partial t} \mathbf{A} + \nabla \bar{\Phi}$.

A. Ginzburg–Landau free energy

Given a constant applied magnetic field H , the conventional Ginzburg–Landau free energy, below the critical transition temperature, is

$$\mathcal{G}(\psi, \mathbf{A}) = \int_{\Omega} \left(\frac{1}{2} \left| \left(\frac{i}{\kappa} \nabla + \mathbf{A} \right) \psi \right|^2 + \frac{1}{4} (1 - |\psi|^2)^2 + \frac{1}{2} |\text{curl } \mathbf{A} - H|^2 \right) d\Omega,$$

where κ , the Ginzburg–Landau parameter, is a material constant representing the ratio of the penetration depth and the coherence length.

Note that for the general three-dimensional (3D) problems, the interactions between the fields inside the superconducting sample and the external field are important. Various measurement of critical fields are also affected by the geometrical shape of the sample.^{72,69,78,85} To apply the Ginzburg–Landau theory in such situations, a coupled system of equations must be solved in both the sample and its exterior. Energetically speaking, in the case where Ω is a bounded domain in 3D, it may be necessary to reformulate the free energy as follows:

$$\mathcal{G}(\psi, \mathbf{A}) = \int_{\Omega} \left(\frac{1}{2} \left| \left(\frac{i}{\kappa} \nabla + \mathbf{A} \right) \psi \right|^2 + \frac{1}{4} (1 - |\psi|^2)^2 \right) d\Omega + \frac{1}{2} \int_{R^3} |\text{curl } \mathbf{A} - H|^2 dR^3.$$

The minimizers of the GL energy functional satisfy the Euler-Lagrange equations, also called the GL equations, of the form

$$\left(\frac{i}{\kappa}\nabla + \mathbf{A}\right)^2 \psi - \psi + |\psi|^2 \psi = 0, \quad (2.1)$$

$$\mathbf{curl} \mathbf{curl} \mathbf{A} + \frac{i}{2\kappa}(\psi^* \nabla \psi - \psi \nabla \psi^*) + |\psi|^2 \mathbf{A} = 0. \quad (2.2)$$

Here, ψ^* is the complex conjugate of ψ . With the present nondimensionalization, $|\psi|=1$ and $|\psi|=0$ correspond to the perfectly superconducting state and the normal state.

This set of nonlinear Ginzburg–Landau equations in the (bounded) interior of Ω is coupled with the linear Maxwell equations in the (unbounded) exterior $\Omega^c = \mathbb{R}^3 \setminus \bar{\Omega}$ with far field conditions at infinity and interface conditions on $\Gamma = \partial\Omega$. If we only consider the interior problem (typically valid for a two-dimensional cross section of a long 3D cylinder with the applied magnetic field perpendicular to the cross section), then on Γ , it is customary to use the natural boundary conditions

$$\left(\frac{i}{\kappa}\nabla \psi + \mathbf{A}\psi\right) \cdot \mathbf{n} = 0, \quad (2.3)$$

$$\mathbf{curl} \mathbf{A} = H. \quad (2.4)$$

More general boundary conditions have also been studied. For instance, to study the proximity effect, one may use

$$\left(\frac{i}{\kappa}\nabla \psi + \mathbf{A}\psi\right) \cdot \mathbf{n} = -i\gamma\psi.$$

We refer to Refs. 14, 43, and 91 for more discussions.

B. Time-dependent Ginzburg–Landau equations

Let η_1 and η_2 be given relaxation parameters, the conventional time-dependent Ginzburg–Landau (TDGL) model is given by

$$\eta_1 \left(\frac{\partial \psi}{\partial t} + i\kappa \bar{\Phi} \psi \right) + \left(\frac{i}{\kappa} \nabla + \mathbf{A} \right)^2 \psi - \psi + |\psi|^2 \psi = 0, \quad (2.5)$$

$$\eta_2 \left(\frac{\partial \mathbf{A}}{\partial t} + \nabla \bar{\Phi} \right) + \mathbf{curl} \mathbf{curl} \mathbf{A} + \frac{i}{2\kappa} (\psi^* \nabla \psi - \psi \nabla \psi^*) + |\psi|^2 \mathbf{A} = 0, \quad (2.6)$$

with boundary conditions

$$\left(\frac{i}{\kappa}\nabla \psi + \mathbf{A}\psi\right) \cdot \mathbf{n} = 0, \quad (2.7)$$

$$\mathbf{curl} \mathbf{A} = H, \quad (2.8)$$

$$\eta_2 \left(\frac{\partial \mathbf{A}}{\partial t} + \nabla \bar{\Phi} \right) \cdot \mathbf{n} = \mathbf{J}_a \cdot \mathbf{n}, \quad (2.9)$$

where \mathbf{J}_a is an applied current. The initial conditions are

$$\psi(\mathbf{x}, 0) = \psi_0(\mathbf{x}) \quad \text{and} \quad \mathbf{A}(\mathbf{x}, 0) = \mathbf{A}_0(\mathbf{x}) \quad \text{in } \Omega.$$

Note that we only focus on the interior problem for now and we assume that η_1 and η_2 are both positive real numbers (dynamics with complex valued η_1 have been studied³⁰).

First, it is convenient to introduce an auxiliary variable $\Phi_a(\mathbf{x}, t) = (\mathbf{J}_a \cdot \mathbf{x}) / \eta_2$ and define $\Phi = \bar{\Phi} - \Phi_a$. The triple (ψ, \mathbf{A}, Φ) is often used as the primary variables for the TDGL equations which are related to the energy functional by

$$\eta_1 \left(\frac{\partial \psi}{\partial t} + i\kappa \bar{\Phi} \psi \right) = - \frac{\partial \mathcal{G}}{\partial \psi}(\psi, \mathbf{A}), \quad (2.10)$$

$$\eta_2 \left(\frac{\partial \mathbf{A}}{\partial t} + \nabla \Phi \right) = - \frac{\partial \mathcal{G}}{\partial \mathbf{A}}(\psi, \mathbf{A}). \quad (2.11)$$

C. Gauge invariance

Both the GL and the TDGL equations enjoy the *gauge invariance* property, see Refs. 32 and 72 for more detailed discussions.

Numerical minimization of the free energy functional is made difficult due to the gauge invariance. However, a nice remedy has been developed to avoid such pitfalls.⁴³ Define

$$\mathcal{F}(\psi, \mathbf{A}) = \mathcal{G}(\psi, \mathbf{A}) + \int_{\Omega} |\operatorname{div} \mathbf{A}|^2 \, d\mathbf{x}. \quad (2.12)$$

By choosing proper gauge transformation, the following can be shown.

Theorem 2.1: *The following minimization problems are equivalent:*

$$\begin{array}{lll} \text{Min } \mathcal{G}(\psi, \mathbf{A}) & \text{Min } \mathcal{G}(\psi, \mathbf{A}) & \text{Min } \mathcal{F}(\psi, \mathbf{A}) \\ \text{s.t. } \psi \in \mathcal{H}^1(\Omega), & \Leftrightarrow \text{s.t. } \psi \in \mathcal{H}^1(\Omega), & \Leftrightarrow \text{s.t. } \psi \in \mathcal{H}^1(\Omega), \\ \mathbf{A} \in \mathbf{H}^1(\Omega) & \mathbf{A} \in \mathbf{H}_n^1(\operatorname{div}, \Omega) & \mathbf{A} \in \mathbf{H}_n^1(\Omega). \end{array}$$

where $\mathbf{H}_n^1(\Omega)$ is a subspace of $\mathbf{H}^1(\Omega)$ with vanishing normal component on the boundary while $\mathbf{H}_n^1(\operatorname{div}, \Omega)$ is a subspace of divergence free vector valued functions in $\mathbf{H}_n^1(\Omega)$.

With the equivalent formulation, one can simply enforce the Coulomb gauge implicitly by solving for the variational problems with respect to \mathcal{F} in $\mathcal{H}^1(\Omega) \times \mathbf{H}_n^1(\Omega)$. The penalty term $\|\operatorname{div} \mathbf{A}\|^2$ serves as a null Lagrangian which vanishes at the energy minimizer.

The TDGL equations (2.10) and (2.11) may be viewed as the gauge invariant gradient flow of the free energy. By examining the various choices of the gauge, the well posedness of the system was first reported in 1992 at the first world congress of nonlinear analysts.^{33,32} Sharper results based on some better energy estimates and the long time solution behavior have later been studied, for instance, in Refs. 72, 90, and 56.

III. NUMERICAL APPROXIMATIONS

Due to the complexity stemming from the full nonlinearity of the GL models, analytical studies have been limited to special cases. Numerical approximations, on the other hand, have provided researchers useful tools to understand the models and to simulate the physical properties of the superconductors. The systematic study of the GL models from the numerical analysis point of view was first made in Ref. 43. Later, many works on the numerical approximations of Ginzburg–Landau type models and their rigorous theoretical analysis have appeared. Here, we briefly discuss the finite difference,^{3,21,26,29,35,55,57,59,61} finite element,^{4,17,20,18,40,43–45,62,93,95} and finite volume methods^{46–48} for spatial discretizations. We also discuss various time-stepping schemes for time-dependent models^{31,79,80} and some parallel and adaptive algorithms.

A. Finite element approximations

The basic theory of conforming finite element approximations for the steady state GL equations in a bounded domain has been presented in Ref. 43. Let us choose a pair of conforming finite element spaces $\mathcal{V}_k^h \times \mathbf{V}_k^h \subset \mathcal{H}^1(\Omega) \times \mathbf{H}_n^1(\Omega)$ where h being a mesh parameter, and assume that they satisfy the approximation properties

$$\inf_{g^h \in \mathcal{V}_k^h} \|\psi - g^h\|_1 \leq ch^r \|\psi\|_{r+1},$$

$$\inf_{\mathbf{B}^h \in \mathbf{V}_k^h} \|\mathbf{A} - \mathbf{B}^h\|_1 \leq ch^r \|\mathbf{A}\|_{r+1}$$

for functions ψ and \mathbf{A} of sufficient regularity.

Then, the discrete Galerkin finite element approximation can be formulated as follows:⁴³

$$\mathbf{Min} \mathcal{F}(\psi^h, \mathbf{A}^h),$$

$$\text{s.t. } (\psi^h, \mathbf{A}^h) \in \mathcal{V}_k^h \times \mathbf{V}_k^h.$$

It has been shown that the above problems generate a sequence of convergent approximate solutions as $h \rightarrow 0$ under the minimal regularity condition. Moreover, optimal order of error estimates of the following type have been derived for nonsingular solution branches:

$$\|\psi - \psi^h\|_1 + \|\mathbf{A} - \mathbf{A}^h\|_1 \leq ch^k \{\|\psi\|_{k+1} + \|\mathbf{A}\|_{k+1}\}.$$

It is worthwhile to note that no inf-sup condition is required for the finite element spaces. The gauge condition is not strictly imposed for finite mesh parameter h , but it is shown to be valid in the limit as $h \rightarrow 0$.

The finite element methods have later been generalized to other related models, such as the d -wave GL equations,⁹³ optimal control of GL models⁶⁰ and the Lawrence-Doniach models for layered superconductors.^{41,62} In Refs. 44 and 45, various numerical simulations have been conducted based on the finite element approximations.

The application of finite element method to TDGL has been considered in Ref. 31. Besides the basic convergence results for semidiscrete scheme, both first order and second in time discretization schemes have also been presented. Let Δt_n be the step size and $(\psi_n^h, \mathbf{A}_n^h)$ the numerical solution at time t_n . When the applied current is absent, the first order backward Euler scheme can be given a variational form, find $(\psi_{n+1}^h, \mathbf{A}_{n+1}^h)$ such that it solves the problem

$$\mathbf{Min} \mathcal{G}_{\Delta t_n}(\psi, \mathbf{A}) = \mathcal{G}(\psi, \mathbf{A}) + \frac{1}{\Delta t_n} \int_{\Omega} [\eta_1 |\psi - \psi_n^h|^2 + \eta_2 |\mathbf{A} - \mathbf{A}_n^h|^2] d\Omega.$$

It turns out that a second order in time scheme can also be similarly formulated, first find $(\psi_*^h, \mathbf{A}_*^h)$ that minimizes

$$\mathcal{G}(\psi, \mathbf{A}) + \frac{1}{2\Delta t_n} \int_{\Omega} [\eta_1 |\psi - \psi_n^h|^2 + \eta_2 |\mathbf{A} - \mathbf{A}_n^h|^2] d\Omega,$$

then we let $(\psi_{n+1}^h, \mathbf{A}_{n+1}^h) = 2(\psi_*^h, \mathbf{A}_*^h) - (\psi_n^h, \mathbf{A}_n^h)$. We note that the derivation of error estimates of the fully discrete scheme was, however, not rigorously provided there. By using a mixed formulation, Ref. 17 has presented a more complete theory for the approximation of the TDGL along with optimal order error estimates in two space dimension. Later, Ref. 20 considered approximations to a related optimal control problem. Generalizations to the time-dependent Lawrence-Doniach model have been presented in Ref. 62.

B. Finite difference approximations

Same as in the approximations of many other physical problems, the finite difference approximations of the GL models have been the most widely used approach. Though conventional difference schemes have been studied in Refs. 55 and 67, much of the focus has been on the gauge invariant difference approximation. The motivation has come from the fact that the underlying physical model enjoys the gauge invariance property. In Ref. 3, a gauge invariant finite difference scheme was proposed for the steady-state GL equations on a uniform rectangular grid, in the spirit of discrete gauge field theory. Many subsequent works have followed up on such an approach via an introduction of the so-called link and bond variables, and various extensions have also been made.^{21,22,55,57,59,61,66,68} For the approximation of the magnetic vector potential, such an approach is naturally related to the idea of staggered grid (marker-and-cell) used in computational electromagnetics and fluid dynamics.

For simplicity, let us consider the two-dimensional setting with a uniform rectangular mesh of grid size h . Following the notation in Ref. 35, the discrete gauge invariant energy functional is given by

$$\mathcal{G}^h(\vec{\psi}, \vec{A}) = \frac{1}{2} \sum_{jk} \frac{1}{\kappa^2} |\psi_k \exp(-i\kappa a_{jk}h) - \psi_j|^2 + \sum_j \frac{h^2}{4} (1 - |\psi_j|^2)^2 + \frac{1}{2} \sum_{jklm} (a_{jk} + a_{kl} + a_{lm} + a_{mj} - Hh)^2, \quad (3.1)$$

where the first sum is over all neighboring edges, the second over all vertices and the third over all square cells. $\vec{\psi} = \{\psi_j\}$ are the approximations of the order parameter at the cell vertices and $\vec{A} = \{a_{jk}\}$ are the approximations of the signed tangential component of the magnetic vector potential at the midpoint of the cell edges.

The gauge invariant backward Euler scheme is given by³⁵

$$\eta_1 \frac{\psi_j^n - \psi_j^{n-1} \exp(-i\kappa \bar{\Phi}_j^n \Delta t)}{\Delta t} = -\frac{1}{h^2} \frac{\partial \mathcal{G}^h}{\partial \psi_j^n}(\vec{\psi}^n, \vec{A}^n)$$

and

$$\eta_2 \left(\frac{a_{jk}^n - a_{jk}^{n-1}}{\Delta t} + \frac{\Phi_k^n - \Phi_j^n}{h} \right) = -\frac{1}{h^2} \frac{\partial \mathcal{G}^h}{\partial a_{jk}^n}(\vec{\psi}^n, \vec{A}^n)$$

for $n=1, 2, \dots, N=T/\Delta t$. Here, $\{\bar{\Phi}_j^n\}$ are the approximations of the scalar electric potential. Note that the equations at the nodes on the boundary may require slight modifications. A complete and rigorous analysis for such a discretization has been provided in Ref. 35, including the proof of the discrete maximum principle, discrete energy law, and optimal order error estimates.

It remains to be seen if a higher order in time fully discrete gauge invariant scheme can be developed for the TDGL equations.

We note here also that, in practical numerical simulations, explicit or semi-implicit in time difference schemes have been mostly employed. In general, these schemes are only conditionally stable at best.

C. Finite volume approximations

As more and more attention is being paid to the study of the effect of the sample geometry and topology on the superconductivity phenomena, methods based on unstructured grids become more competitive in such cases. Besides the finite element methods we have discussed, finite volume methods have also been developed which have the combined advantage of being able to work with an unstructured grid while preserving the discrete gauge invariance.^{48,46,47}

A standard extension to the staggered grid used in the gauge invariant difference approximation is the Voronoi-Delaunay pair. Given a set of distinct points $\{x_j\}_{j=1}^n \subset \mathbb{R}^2$, we can define for each point $x_j, j=1, \dots, n$, the corresponding Voronoi region $V_j, j=1, \dots, n$, by

$$V_j = \{\mathbf{y} \in \mathbb{R}^2 \mid |x_j - \mathbf{y}| < |x_k - \mathbf{y}| \text{ for } 1 \leq k \leq n \text{ and } k \neq j\}.$$

We refer to $\{V_j\}_{j=1}^n$ as the *Voronoi tessellation* corresponding to the generators $\{x_j\}_{j=1}^n$. The dual tessellation to a Voronoi tessellation consisting of triangles is referred to as a *Delaunay triangulation*. Given a discrete vector field \vec{A} tangentially defined at the midpoints of the triangle edges of a Delaunay triangulation, it is easily seen that such vectors are normal to the edges of the Voronoi regions. Thus, discrete calculus can be defined for the curl operator on the Delaunay triangles and for the div operator on the Voronoi cells.

Then, the central idea for finding a suitable discretization of the GL energy functional is to construct a gauge invariant approximation to $|\nabla\psi - i\kappa\mathbf{A}\psi|$. It was noticed in Ref. 48 that one may first project the vector $v = \nabla\psi - i\kappa\mathbf{A}\psi$ into the tangential components along the triangle edges and obtain the following simple identity

$$|\tau_{ijk}|v|^2 = \sum \cot \theta_i |v \cdot (x_j - x_k)|^2,$$

where the sum is over all three edges and θ_i is the opposite angle. Notice that if we let θ_{i1} and θ_{i2} be the two opposing angles corresponding to the same edge $x_j x_k$, then

$$\cot \theta_{i1} + \cot \theta_{i2} = \frac{|\Gamma_{jk}|}{|x_j - x_k|},$$

where Γ_{jk} is the common edge between the two adjacent Voronoi regions V_{i1} and V_{i2} . Now, $|v \cdot (x_j - x_k)|$ can be approximated by $|\psi_k \exp(-i\kappa a_{jk}|x_j - x_k|) - \psi_j|$.

Thus, the Ginzburg–Landau functional is discretized as follows:⁴⁸

$$\begin{aligned} \mathcal{F}^h(\vec{\psi}^h, \vec{A}^h) = & \sum_{j=1}^n \frac{1}{4|V_j|} (1 - |\psi_j|^2)^2 + \sum_{j=1}^n \left\{ \sum_{k \in \chi_j} \frac{|\Gamma_{jk}|}{2\kappa^2 |x_j - x_k|} |\psi_k \exp(-i\kappa a_{jk}|x_j - x_k|) - \psi_j|^2 \right\} \\ & + \sum_{\tau_{jkl}} \frac{1}{2\tau_{jkl}} (a_{jk}h_{jk} + a_{kl}h_{kl} + a_{lj}h_{lj} - H\tau_{jkl})^2, \end{aligned} \quad (3.2)$$

where for any j , the index set χ_j denotes the indices of all vertices which are adjacent to the vertex \mathbf{x}_j . The discrete gauge invariance is understood in the sense that

$$\mathcal{G}^h(\vec{\psi}^h, \vec{A}^h) = \mathcal{G}^h(T_\phi^h(\vec{\psi}^h, \vec{A}^h)),$$

where the transformation T^h is defined by the map

$$\psi_j \rightarrow \psi_j e^{i\kappa\phi_j}, \quad a_{jk} \rightarrow a_{jk} + \frac{\phi_k - \phi_j}{|x_j - x_k|},$$

corresponding to any scale field $\vec{\phi}^h$.

The gauge invariant difference approximation on a rectangular grid discussed earlier is in fact a special case of the above finite volume scheme. This can be seen by making the equivalence of the rectangular cells with the Voronoi cells and the equivalence of the dual cells with pairs of right Delaunay triangles sharing a common edge opposing the right angles.

Similar to the technique introduced in Ref. 43 and in the finite difference setting, a modified functional can be defined to enforce the gauge choice implicitly. Let us define

$$\mathcal{F}^h(\vec{\psi}^h, \vec{A}^h) = \mathcal{G}^h(\vec{\psi}^h, \vec{A}^h) + \sum_j \frac{1}{|V_j|} \left(\sum_{k \in \chi_j} a_{kj} |\Gamma_{kj}| \right)^2.$$

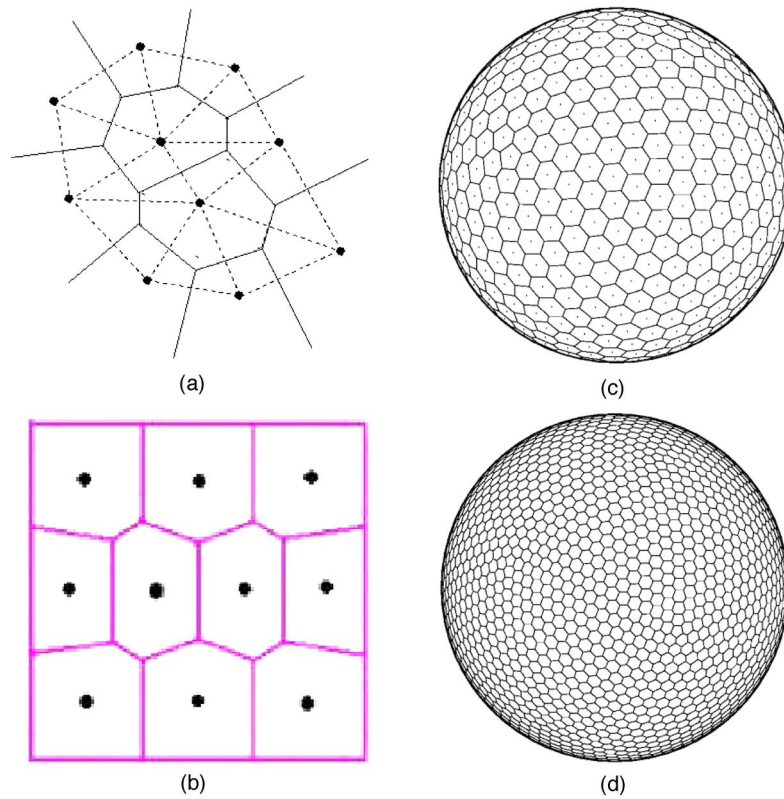


FIG. 1. (Color online) A planar Voronoi-Delaunay pair, a CVT in a square and two SCVTs of different resolution.

Then, it is easy to show that the minimizer of \mathcal{F}^h is also a minimizer of \mathcal{G}^h and it is also divergence free in the discrete sense:

$$\sum_{k \in \chi_j} a_{kj} |\Gamma_{kj}| = 0, \quad \forall j.$$

Moreover, it has been shown that the minimizer of \mathcal{F}^h satisfies the discrete maximum principle, $|\psi_j| \leq 1$ for all j . This, coupled with suitable energy estimates, leads to the convergence of the discrete approximations as the mesh size goes to zero.⁴⁸

In Refs. 46 and 47, such finite volume scheme was extended to solve a reduced set of TDGL models defined on a thin spherical shell. In addition to the basic convergence properties, a feature of the discussions in Refs. 46 and 47 is the consideration of a special Voronoi-Delaunay pair, namely, the spherical centroidal Voronoi tessellations and the corresponding Delaunay triangulations,⁴² see Fig 1. The SCVTs are natural extensions of the centroidal Voronoi tessellations in Euclidean spaces.³⁹ It has been shown that by using the SCVTs, the discrete approximations exhibit a higher order convergence comparing with the conventional Voronoi-Delaunay pair.

Detailed numerical simulations have also been performed in Refs. 46 and 47 using the SCVT based gauge invariant finite volume scheme. Both static vortex configurations and vortex dynamics under applied current have been studied.

D. Artificial boundary conditions

For a full three-dimensional simulation of the GL model, taking into account the effect of the induced magnetic field of the superconducting sample on the field exterior to the sample, the numerical solution of the Ginzburg–Landau equations in the superconducting sample needs to be solved in conjunction with the solution of the Maxwell equations in the exterior.

To overcome the unboundedness of the exterior domain, approximations must be introduced or alternative formulations must be considered. The crudest but often very effective approximation is simply to ignore the effect in the exterior completely. Such approximations are particularly valid for high-kappa materials (in such cases, some reduced GL models have been proposed and used in numerical simulations of vortex lines.^{15,25,40}

As an alternative, a rigorous theory based on artificial boundary conditions has been presented in Ref. 51 to transform the computation domain to a finite ball enclosing the superconducting sample.

The key step is to note that the magnetic energy $\|\text{curl } \mathbf{A}\|_{L^2(\mathbb{R}^3)}^2$, coupled with the null-Lagrangian term $\|\text{div } \mathbf{A}\|_{L^2(\mathbb{R}^3)}^2$ used to enforce the Coulomb gauge, is equivalent to $\|\nabla \mathbf{A}\|_{L^2(\mathbb{R}^3)}^2$ which can be decomposed as $\|\nabla \mathbf{A}\|_{L^2(B_r)}^2 + \|\nabla \mathbf{A}\|_{L^2(B_r^e)}^2$. Here B_r denotes a ball of radius r and $B_r^e = \mathbb{R}^3 \setminus B_r$ denotes its exterior.

For \mathbf{A} 's that are harmonic in B_r^e , we have

$$\|\nabla \mathbf{A}\|_{B_r^e}^2 = \int_{S_r} \mathbf{A} \frac{\partial \mathbf{A}}{\partial \mathbf{n}} dS = \int_{S_r} \mathbf{A} J(\mathbf{A}) dS,$$

where S_r denotes the sphere of radius r , J is the Steklov-Poincaré operator (or the Dirichlet to Neumann map). Since J can be explicitly expressed with the help of Legendre functions, various orders of approximations can be constructed.

Briefly, let the Legendre polynomial and Legendre function be given by

$$P_n^0(t) = P_n(t) = \frac{1}{2^n n!} \frac{d^n (t^2 - 1)^n}{dt^n}, \quad P_n^m(t) = (1 - t^2)^{m/2} \frac{d^m}{dt^m} P_n(t),$$

and let

$$G(\gamma) = -\frac{1}{4\pi R^3} - \sum_{n=1}^{\infty} \frac{(n+1)(2n+1)}{4\pi R^3} P_n(\cos \gamma),$$

for γ defined by $\cos \gamma = \cos \theta \cos \theta' + \sin \theta \sin \theta' \cos(\varphi - \varphi')$ for a pair of points $x = (r, \theta, \varphi)$ and $y = (r, \theta', \varphi')$. Then, with \mathbf{A}_0 satisfying $\text{curl } \mathbf{A}_0 = H$, we have the following equivalent form of the energy functional⁵¹

$$\begin{aligned} \mathcal{F}(\psi, \mathbf{A}) &= \int_{\Omega} \frac{1}{4} (1 - |\psi|^2)^2 d\Omega + \frac{1}{2} \int_{\Omega} \left| \left(\frac{i}{\kappa} \nabla + \mathbf{A} + \mathbf{A}_0 \right) \psi \right|^2 d\Omega + \frac{1}{2} \int_{B_r} |\nabla \mathbf{A}|^2 dx \\ &+ \int_{S_r} \int_{S_r} \mathbf{A}(x) \cdot G(\gamma) I \cdot \mathbf{A}(y) dx dy. \end{aligned}$$

In a nut-shell, the exterior energy is now effectively transformed into an energy defined on the boundary of the ball.

Various approximations of the boundary energy can be made, for instance, using a finite element discretization in the interior of B_r , the following discrete problem has been considered in Ref. 51:

$$\begin{aligned} \mathcal{F}(\psi^h, \mathbf{A}^h) &= \frac{1}{2} \int_{\Omega} \left| \left(\frac{i}{\kappa} \nabla + \mathbf{A}^h + \mathbf{A}_0 \right) \psi^h \right|^2 d\Omega + \int_{\Omega} \frac{1}{4} (1 - |\psi^h|^2)^2 d\Omega + \frac{1}{2} \int_{B_r} |\nabla \mathbf{A}^h|^2 dx \\ &+ \sum_{n=1}^N \frac{(n+1)(2n+1)}{4\pi r^3} \int_{S_r} \int_{S_r} \mathbf{A}^h(x) P_n(\cos \gamma) \mathbf{A}^h(y) dx dy. \end{aligned}$$

Let $r_1 = \text{diam}(\Omega)$, under the approximation assumptions on the finite element spaces made earlier, the following has been proved.

Theorem 3.1: *For a smooth exact solution on a nonsingular solution branch, the approximate solutions satisfy the following error estimates: for h small and $r > r_1$,*

$$\|\psi - \psi^h\|_{1,\Omega} + \|\mathbf{A} - \mathbf{A}^h\|_{1,B_r} \leq c_1 h^k (\|\psi\|_{k+1,\Omega} + \|\mathbf{A}\|_{k+1,B_r}) + c_2(\Omega, r) (r_1/r)^N \|\mathbf{A}\|_{1,B_r},$$

for some constants c_1 and $c_2 = c_2(\Omega, r)$ independent of h and N .

It has been seen in numerical computation that in practice with $N=6$, it is sufficient to choose the computational domain with r no more than twice the diameter of Ω in order to obtain good accuracy of the approximation in the exterior domain.⁵¹

E. More on time discretization

For TDGL models, while most of the rigorous mathematical analysis have been focused on the fully implicit in time discretizations, explicit marching schemes and semi-implicit marching schemes⁹⁴ have also been frequently used in numerical simulations due to their simplicity in implementation.

Theoretically, to make the time-marching more efficient, other useful ideas have also been considered in the literature. For example, a linearized crank-Nicolson scheme has been considered in Ref. 79, similar to the semi-implicit approach. Analytical studies of an alternating marching scheme have also been made in Ref. 80 where for the order parameter and magnetic potential are solved in alternating steps and thus reducing the size of the implicit nonlinear system by half.

To effectively solve the nonlinear and linear systems employed in the implicit schemes, constructions of suitable preconditioners can be very helpful. In this regard, the Sobolev gradient methods studied in Refs. 82 and 83 fit into such a framework. Essentially, the gradient flows in the H^{-1} space considered there are equivalent to employing the inverse of Laplace operator Δ^{-1} as the preconditioner for the standard gradient flow in the L^2 space.

For high values of κ , the Ginzburg–Landau parameter, the original GL models can often be simplified. A particular simplification corresponding to high applied magnetic field has been considered in Refs. 15 and 40. The reduced equations are very much similar to the so-called Gross-Pitaevskii equations used to model the BEC superfluid.⁵ In Ref. 9, a class of efficient splitting schemes for computing the ground state solutions of the BEC condensate based on the normalized gradient flow has been studied which may be readily applied to the solution of the reduced GL models.

F. Multilevel, adaptive and parallel algorithms

The numerical simulations of the vortex state in type-II superconductors based on the GL models become computationally challenging when there is a need to resolve a large number of vortices. More efficient implementations of the numerical schemes thus become necessary. There have been a lot of interesting attempts made along this direction. For example, multilevel finite element methods have been analyzed in Ref. 63 for a d -wave GL model, following earlier works of Refs. 36 and 93. Posterior error estimates and adaptive finite element methods have been studied in Refs. 18 and 64 with both rigorous analysis and numerical examples.

Parallelization is naturally another important avenue for greater computational efficiency. In Ref. 59, parallelized MPI-based implementation of the explicit finite difference discretization schemes has been presented along with many large scale simulations. Using a natural domain decomposition strategy, a number of parallel algorithms for the simulation of layered superconductors based on the Lawrence Doniach model have been studied in Ref. 41. The implementation has been made first using PVM, with an MPI version developed subsequently. Numerical results indicated significant speed-ups and good scalability. Moreover, interesting numerical simulations of three-dimensional vortex tubes, their dynamics and pinning effect have been made there as well.

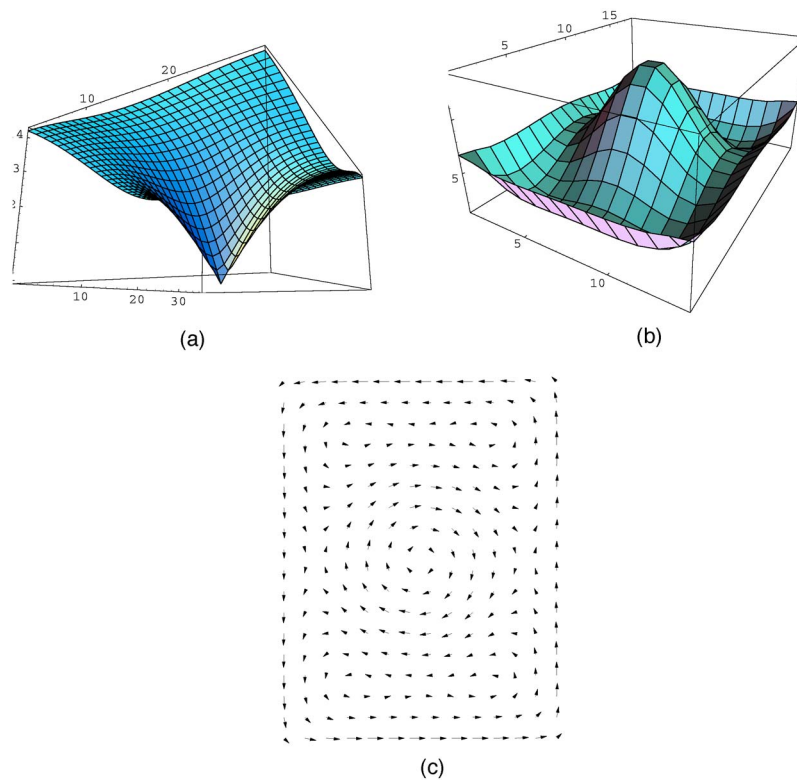


FIG. 2. (Color online) Magnitude of the order parameter, induced field and supercurrent in a 2D rectangular domain.

IV. NUMERICAL SIMULATIONS AND OTHER COMPUTATIONAL ISSUES

We now briefly describe some results of numerical simulations conducted throughout the last decade. These are based on either the finite element codes or the finite volume codes discussed earlier. We refer to Refs. 4, 23–25, 38, 46, and 47 for additional simulations.

A. Vortex solutions

A well-known feature of superconductivity is the phenomena of quantized vortices. For type-II superconductors, the study of Abrikosov on the vortex lattices based on the GL models has become a seminal work that exhibits the great predictive power of the GL theory.

In Fig. 2, we present a few typical plots for the numerical solutions of the steady state GL equations which include a surface plot of the magnitude of the order parameter, a surface plot of the induced magnetic field given by $\text{curl } \mathbf{A}$ and a vector plot of the superconducting current. The solution corresponds to one with a single vortex at the center of a rectangular superconducting sample.⁴

More systematic analysis and simulations of the phase transitions, vortex nucleation, and critical fields can be found in, for instance, Refs. 4, 7, 8, 11, 12, 65, 72, 85, 89, and 88, and the references cited therein.

B. Pinning of vortices in superconducting sample

One of the more intriguing features of superconductivity is the effect of vortex pinning which preserves the superconducting properties in a superconductor despite the penetration of the applied magnetic field.

The GL models have been used to study the pinning effect from many different angles, for instance, pinning due to variable thickness in thin films,^{13,27,28,72} spatial inhomogeneities and

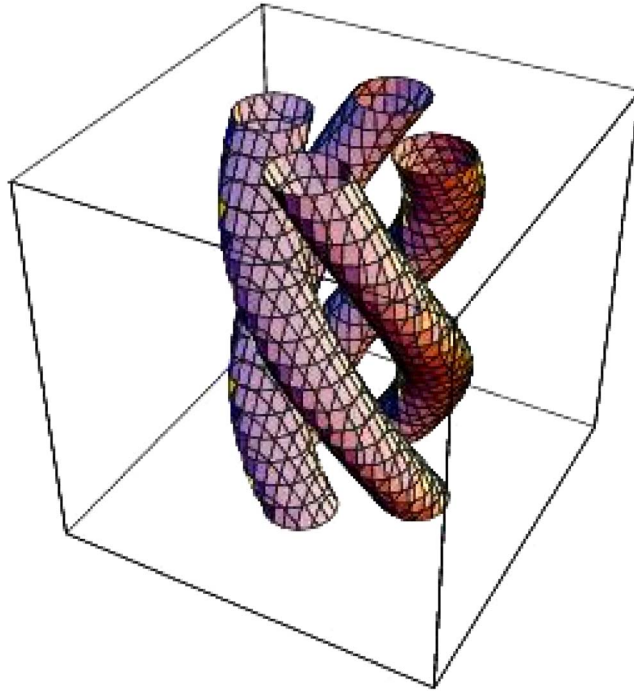


FIG. 3. (Color online) Isosurface plot of vortex tubes pinned in a 3D sample.

normal inclusions and anisotropy.^{14,25,49,50} In Fig. 3, three-dimensional vortex tubes pinned by normal inclusions are shown which were computed via the Lawrence-Doniach variant of the GL model in Ref. 41. Due to the collective pinning force, the vortex tubes are no longer strictly aligned in the direction of the applied magnetic field.

C. Vortex state in a thin superconducting spherical shell

The geometry of spherical shell is not only used in superconductivity applications, but also provides an ideal setting for one to examine the vortex state.

With increasing values of the applied magnetic field, some of the energy minimizing superconducting and vortex solutions are given in Fig. 4. We refer to Ref. 46 for more detailed descriptions of the corresponding parameter values.

In Fig. 5, minimum energy values $\mathcal{G}(H)$ corresponding to different external magnetic field strengths H are plotted, along with the magnetization curve given by the derivatives of minimum energy $\mathcal{G}(H)$.

The spatially homogeneous applied magnetic field naturally produces vortices of opposite signs on the two hemispherical shells, thus providing a window for us to see the details of vortex nucleation and vortex annihilation (see Ref. 10 for some analysis in a simpler setting). In Fig. 6, with the applied magnetic field aligned along the poles, the density plots of order parameter show that a pair of vortices of opposite signs first nucleate near the equator, then later split and move into the interior of the hemispheres.⁴⁶

Other simulations on vortex annihilation can be found in Ref. 40 in the planar domain, aided by an applied current.

D. Vortex motion driven by an applied current

An applied current J generally exerts a Lorentz force $F=J\times B$ on each vortex core such that the motion of vortices would induce an electric field, and thus produces electrical resistance. Thus,

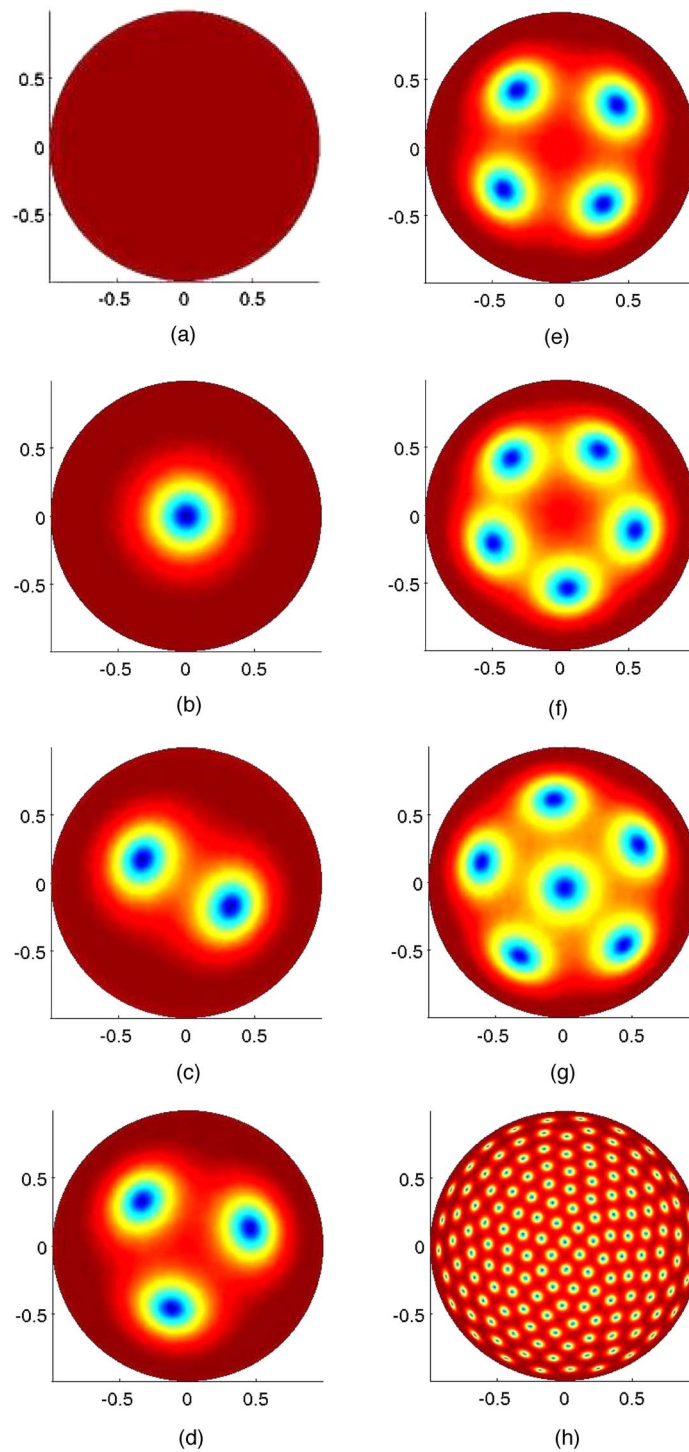


FIG. 4. (Color online) Energy minimizing vortex configurations on the upper hemisphere.

in superconductivity, it is important to understand the interaction of the vortices with the applied current and study the critical values of the applied current which will dislodge the vortices from their equilibrium positions.

In Fig. 7, contour plots of the order parameter are given, corresponding to solution of the

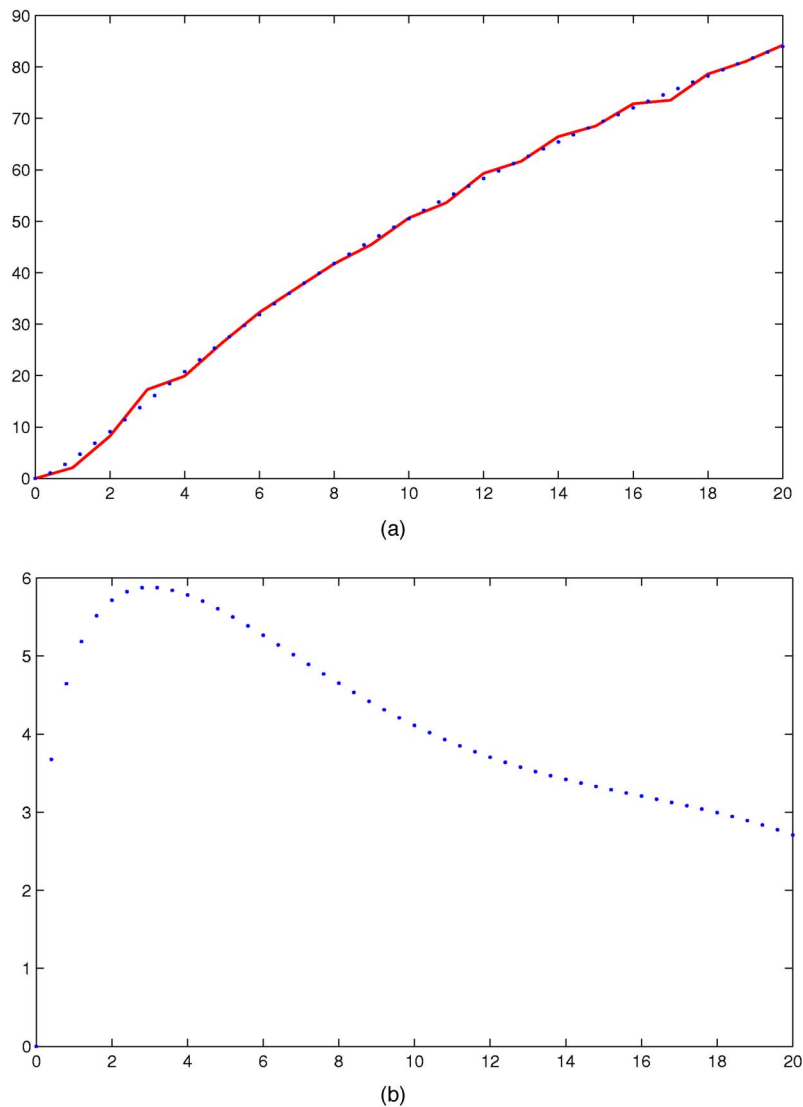


FIG. 5. (Color online) Minimum energy values with its polynomial fitting and the magnetization curve.

TDGL in a two-dimensional square with a constant applied current imposed along the vertical direction. A single vortex starts to move from the left to the right due to the Lorentz force.

E. Effect of thermal fluctuation

The effect of thermal fluctuations play a central role on the pinning of vortices in type-II superconductors. In Refs. 23 and 24, such effects have been examined through stochastic variants of a time-dependent Ginzburg–Landau model valid for high values of the Ginzburg–Landau parameter. Both additive and multiplicative noise variants have been considered. Many numerical computations have been presented that illustrate the effects that noise has on the dynamics of vortex nucleation and vortex motion. In Fig. 8, isosurface plots of vortex tubes are presented corresponding to different values of variance of the additive noise term using for the simulation of Langevin dynamics. The snapshots are taken at the same time instant and the vortex lattice melting effect can be observed in the process.

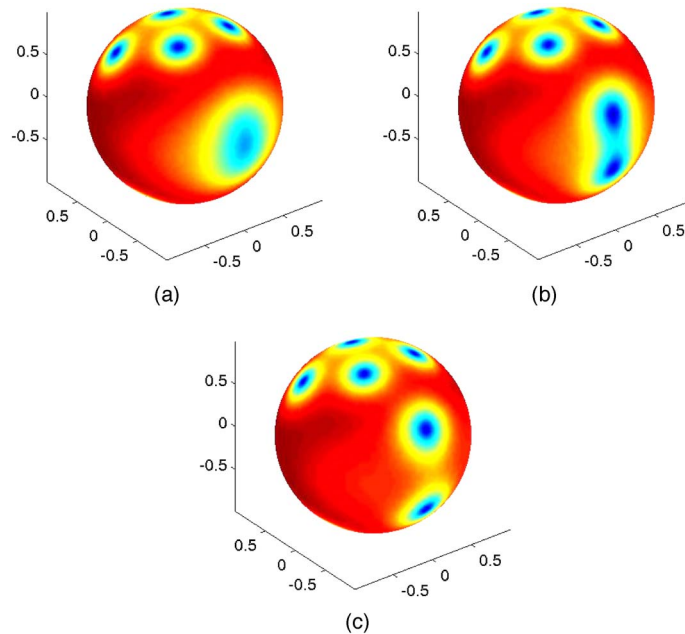


FIG. 6. (Color online) The nucleation and the splitting of vortex pairs near the equator.

F. Variants of Ginzburg–Landau models

The great success of the Ginzburg–Landau models for low T_c superconductivity generated tremendous interests in extending them to other settings including layered materials and high T_c superconductors. For example, in Ref. 36, simulations of a d -wave GL model have been carried out, the vortex solutions there typically display a fourfold symmetry. In certain parameter regimes, the basic stability properties of single and multiple vortices deviated significantly from the single component counterpart, see Fig. 9 for an illustration of a stable double vortex profile.

More analytical and numerical studies of d -wave GL models can be found in Refs. 73, 86, and 93. Numerical studies of other extensions of the GL models have also been performed, for instance, see Ref. 6 for simulations based on the SO(5) model.

Related to the vortex state in superconductors, the 1995 experimental confirmation of Bose-Einstein condensation (BEC) in alkali-metal gases provides another avenue to study the phenomena of quantized vortices. In recent BEC experiments, vortices have been nucleated with the help of laser stirring and rotating magnetic traps. Remarkably, many of the phenomenological properties of quantized vortices have been well captured by mathematical models such as the Gross-Pitaevskii (GP) equations. In the case of rotating magnetic traps, the mathematical form of the GP

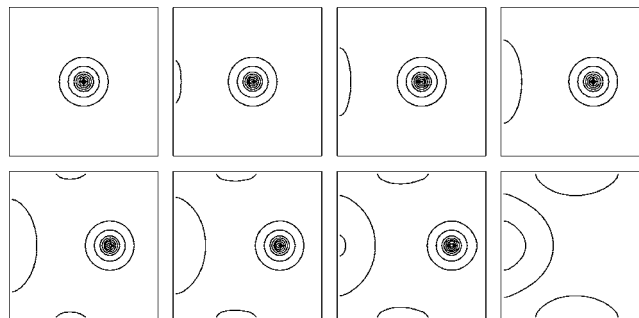


FIG. 7. Motion of vortices in the presence of an applied current.

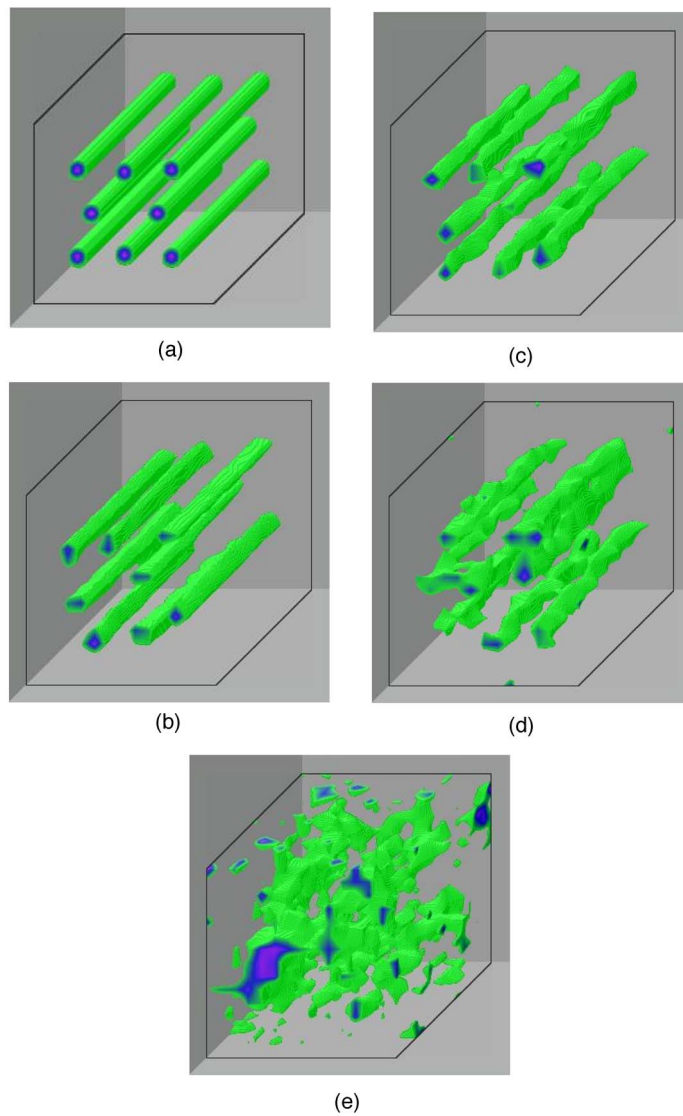


FIG. 8. (Color online) Snapshots of the vortex tubes in a cubic sample with increasing additive noises.

equations have close resemblance with the high-kappa Ginzburg–Landau (GL) model.⁴⁰ Utilizing the mathematical theory and the numerical codes developed for the GL,⁵ presented a similar mathematical framework for rigorously characterizing the critical velocities for the vortex nucleation in a BEC cloud subject to a rotating magnetic trap. A class of splitting schemes for com-

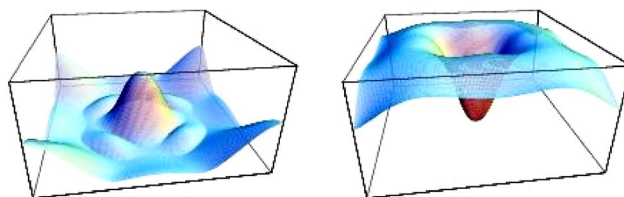


FIG. 9. (Color online) Surface plots of the s and d wave density for a double vortex profile in a GL $s+d$ model.

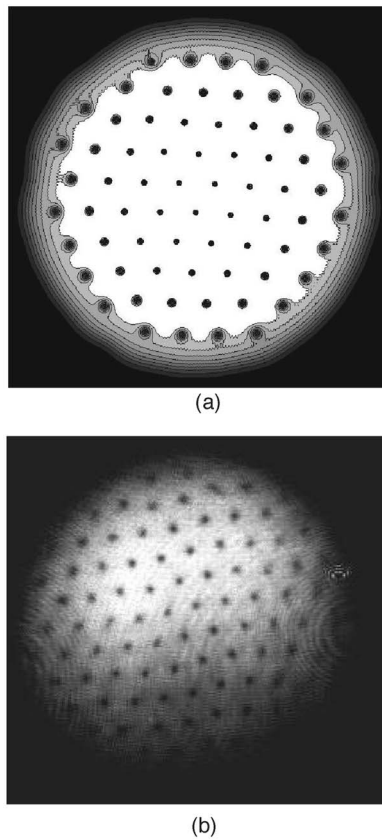


FIG. 10. Vortices in BEC: our numerical simulation (left) vs the MIT experiment (right) (Ref. 1).

puting the ground state solutions of the BEC condensate based on the normalized gradient flow has also been presented.⁹ In Fig. 10, we provide a particular comparison of experimental pictures and the result of numerical simulations of the vortex solution with parameters taken from the experimental values based on the code developed in Ref. 5.

G. Computational challenges

The interests of the vortex state not only lie in the study of the vortex structures for a few isolated vortices, but also in the study of the collective effect of a large number of vortices and vortex lattices and their interactions with material structure and defects as well as the impact of sample topology and geometry. Simulations of GL models have been performed recently on structures like buckyballs and for MgB2 thin films. (See Fig. 11.)

In practice, numerical simulations of exceedingly large numbers of vortices based on the GL models remain computationally challenging, partly due to the intriguing properties associated with the vortex quantization effect. More specifically, for a square sample with n vortices in the interior, the phase angle of the complex order parameter will endure a change of $2n\pi$ around the boundary of the sample. If m points are needed to resolve a single period of phase winding, then $mn/4$ points will roughly be needed on each edge of the square. Thus, a uniform mesh will require up to $m^2n^2/16$ grid points. For large n and even moderate values of m , this can become very demanding computationally even for two-dimensional problems, not to mention the more challenging three-dimensional cases.

Naturally, adaptive schemes may save the computational cost significant, but with densely packed vortices, refinement may be required almost everywhere, and their efficiency are thus reduced. In particular, we note that it is not sufficient to only refine near the vortex cores as the

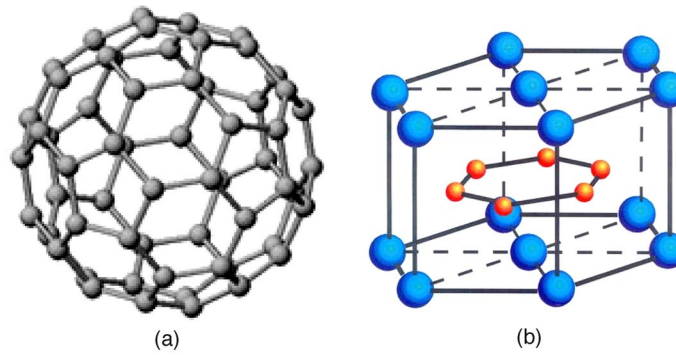


FIG. 11. (Color online) A buckyball and the atomic structure of MgB₂.

correct resolution of the highly oscillatory phase change is also very important, see Fig. 12 for an interesting illustration on how the real and imaginary parts of the order parameter behave in comparison with the magnitude for a solution with 22 pairs of vortices in a spherical shell simulation.⁴⁷ Resolving the highly oscillatory phase for the Ginzburg–Landau simulation is a challenge that can be compared with resolving the solution of the Helmholtz equation with high frequency. In addition, it is easy to see that the variation in the phase variable starts to become increasingly dramatic when getting closer to the boundary (equator). How to effectively tackle such solution behavior remains to be investigated.

On the other hand, for high- T_c superconductors, codes for mesoscale GL models cannot hope to be of direct use in the design of devices due to the presence of a large number of vortices. Whenever computational or analytical results are used in such an environment, they are based on simple homogenized or macroscopic models.

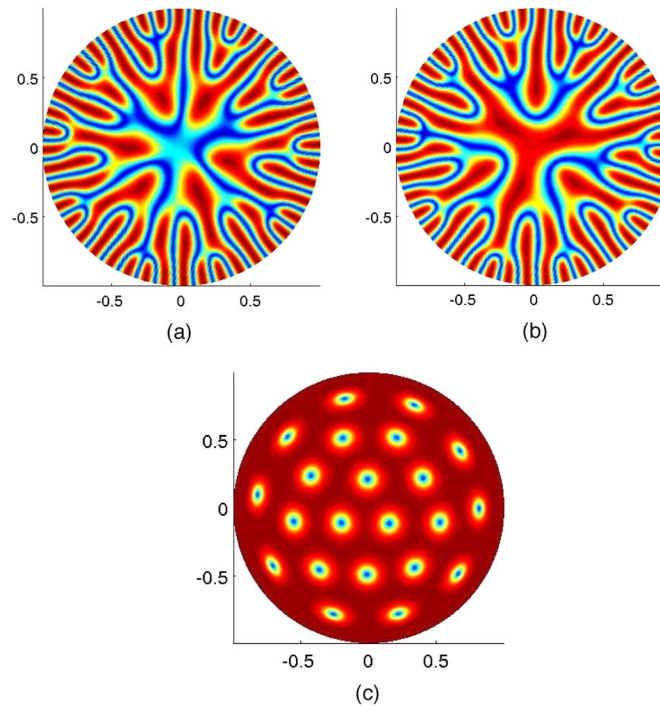


FIG. 12. (Color online) The absolute value of the real (left) and imaginary (center) parts of ψ and the magnitude $|\psi|$.

Recently, mean field models have been derived to describe the vortex state using a vortex density ω . These models are closely related to the GL models as one normally first derives a discrete set of motion laws for individual vortices based on the GL dynamics and a vortex density model is then derived when the number of vortices becomes large.^{16,53,71,81,87} Let u denote the averaged magnetic field, a simplest two-dimensional version of such a model is given by

$$u - \lambda^2 \Delta u = \omega \quad \text{in } \Omega \times (0, T),$$

$$\omega_t - \nabla \cdot (\omega \nabla u) = 0 \quad \text{in } \Omega \times (0, T),$$

with suitable initial and boundary conditions. There have been a lot of studies made both from analytical and computational aspects^{19,37,38,52,54,74} in recent years. It is perceivable that more efficient simulation schemes on the vortex state can be developed with a multiscale approach that combines GL model or vortex dynamic laws and the mean field models together. (Also see Refs. 34, 70, 75–77, 84, and 92.)

V. CONCLUSION

Superconductivity is one of the grand challenges identified as being crucial to future economic prosperity and scientific leadership. In this paper, various methods for the numerical approximations of the Ginzburg–Landau models of superconductivity are discussed, with an emphasis on the application to the study of vortex dynamics.

From a practical point of view, large-scale numerical simulations of the magnetic vortices complement physical experiments due to the complex three-dimensional, time-dependent, stochastic and multiscale nature of the phenomena. Thus, the development and analysis of efficient and reliable numerical algorithms remain important tasks. These algorithms and codes may ultimately prove to be useful to physicists and engineers in their study of superconducting phenomena and other related problems such as the BEC superfluidity.

ACKNOWLEDGMENTS

This work is supported in part by Grants Nos. NSF-DMS0409297 and NSF-ITR0205232. The author wishes to thank Max Gunzburger and many other friends and collaborators for their teaching and doing joint works together on the subject over the years. A partial list of them is provided in the references.

- ¹Abo-Shaeer, J., Raman, C., Vogels, J., and Ketterle, W., “Observation of vortex lattices in Bose-Einstein condensates,” *Science* **292**, 476–479 (2001).
- ²Abrikosov, A., “On the magnetic properties of superconductors of the second group,” *Sov. Phys. JETP* **5**, 1174–1182 (1957).
- ³Adler, S. and Piran, T., “Relaxation methods for gauge field equilibrium equations,” *Rev. Mod. Phys.* **56**, 1–40, (1984).
- ⁴Aftalion, A. and Du, Q., “The bifurcation diagram for the Ginzburg–Landau system for superconductivity,” *Physica D* **163**, 94–105 (2001).
- ⁵Aftalion, A. and Du, Q., “Vortices in the Bose-Einstein condensate: The critical velocities and energy diagrams in the Thomas-Fermi regime,” *Phys. Rev. A* **64**, 063603(1-11) (2001).
- ⁶Alama, S., Berlinsky, A. J., Bronsard, L., and Giorgi, T., “Vortices with antiferromagnetic cores in the SO(5) model of high-temperature superconductivity,” *Phys. Rev. A* **60**, 6901–6906 (1999).
- ⁷Baelus, B. and Peeters, F., “Dependence of the vortex configuration on the geometry of mesoscopic flat samples,” *Phys. Rev. B* **65**, 104515 (2002).
- ⁸Baelus, B., Peeters, F., and Schweigert, V., “Saddle-point states and energy barriers for vortex entrance and exit in superconducting disks and rings,” *Phys. Rev. B* **63**, 144517 (2001).
- ⁹Bao, W. and Du, Q., “Computing the ground state of the BEC via normalized gradient flow,” *SIAM J. Sci. Comput. (USA)* **25**, 1674–1697 (2004).
- ¹⁰Bauman, P., Chen, C., Phillips, D., and Sternberg, P., “Vortex annihilation in nonlinear heat flow for Ginzburg–Landau systems,” *Eur. J. Appl. Math.* **6**, 115–126 (1995).
- ¹¹Bauman, P., Phillips, D., and Tang, Q., “Stable nucleation for the Ginzburg–Landau system with an applied magnetic field,” *Arch. Ration. Mech. Anal.* **142**, 1–43 (1998).
- ¹²Bernoff, A. and Sternberg, P., “Onset of superconductivity in decreasing fields for general domains,” *J. Math. Phys.* **39**, 1272–1284 (1998).
- ¹³Chapman, S., Du, Q., and Gunzburger, M., “A variable thickness thin film model for superconductivity,” *ZAMP* **47**,

- 410–431 (1995).
- ¹⁴Chapman, S., Du, Q., Gunzburger, M., “A Ginzburg–Landau type model of superconducting/normal junctions including Josephson junctions,” *Eur. J. Appl. Math.* **6**, 97–114 (1995);
 - ¹⁵Chapman, S., Du, Q., Gunzburger, M., and Peterson, J., “Simplified Ginzburg–Landau models for superconductivity valid for high kappa and high fields,” *Adv. Math.* **5**, 193–218 (1995).
 - ¹⁶Chapman, S., Rubinstein, J., and Schatzman, M., “A mean-field model of superconducting vortices,” *Eur. J. Appl. Math.* **7**, 97–111 (1996).
 - ¹⁷Chen, Z., “Mixed finite element methods for a dynamical Ginzburg–Landau model in superconductivity,” *Numer. Math.* **76**, 323–353 (1997).
 - ¹⁸Chen, Z. and Dai, S., “Adaptive Galerkin method with error control for a dynamical Ginzburg–Landau model in superconductivity,” *SIAM (Soc. Ind. Appl. Math.) J. Numer. Anal.* **38**, 1961–1985 (2001).
 - ¹⁹Chen, Z. and Du, Q., “A non-conforming finite element methods for a mean field model of superconducting vortices,” *Math. Modell. Numer. Anal.* **34**, 687–706 (2000).
 - ²⁰Chen, Z. and Hoffmann, K., “Numerical solutions of an optimal control problem governed by a G-L model in superconductivity,” *Numer. Funct. Anal. Optim.* **19**, 737–757 (1998).
 - ²¹Coskun, E. and Kwong, M., “Simulating vortex motion in superconducting films with the time-dependent Ginzburg–Landau equations,” *Nonlinearity* **10**, 579–593 (1997).
 - ²²Crabtree, G., Leaf, G., Kaper, H., Vinokur, V., Koshelev, A., Braun, D., Levine, D., Kkwok, W., and Fendrich, J., “Time-dependent Ginzburg–Landau simulations of vortex guidance by twin boundaries,” *Physica C* **263**, 401–408 (1996).
 - ²³Deang, J., Du, Q., and Gunzburger, M., “Stochastic dynamics of the Ginzburg–Landau vortices,” *Phys. Rev. B* **64**, 52506–52510 (2001).
 - ²⁴Deang, J., Du, Q., and Gunzburger, M., “Modeling and computation of random thermal fluctuations and material defects in the Ginzburg–Landau model for superconductivity,” *J. Comput. Phys.* **181**, 45–67 (2002).
 - ²⁵Deang, J., Du, Q., Gunzburger, M., and Peterson, J., “Vortices in superconductors: Modeling and computer simulations,” *Philos. Trans. R. Soc. London, Ser. A* **355**, 1957–1968 (1997).
 - ²⁶Demachi, K., Yoshida, Y., Asakura, H., and Miya, K., “Numerical analysis of magnetization processes in type II superconductors based on Ginzburg–Landau theory,” *IEEE Trans. Magn.* **32**, 1156–1159 (1996).
 - ²⁷Ding, S. and Du, Q., “Critical magnetic field and asymptotic behavior for superconducting thin films,” *SIAM J. Math. Anal.* **34**, 239–256 (2002).
 - ²⁸Ding, S. and Du, Q., “The global minimizers and vortex solutions to a Ginzburg–Landau model of superconducting films,” *Commun. Pure Appl. Anal.* **1**, 327–340 (2002).
 - ²⁹Doria, M., Gubernatis, J., and Rainer, D., “Solving the Ginzburg Landau equations by simulated annealing,” *Phys. Rev. B* **41**, 6335–6340 (1990).
 - ³⁰Dorsey, A., “Vortex motion and the Hall effect in type-II superconductors: A time-dependent Ginzburg–Landau theory approach,” *Phys. Rev. B* **46**, 8376–8392 (1992).
 - ³¹Du, Q., “Finite element methods for the time dependent Ginzburg–Landau model of superconductivity,” *Comput. Math. Appl.* **27**, 119–133 (1994).
 - ³²Du, Q., “Global existence and uniqueness of solutions of the time-dependent Ginzburg–Landau equations in superconductivity,” *Appl. Anal.* **52**, 1–17 (1994).
 - ³³Du, Q., “Time dependent Ginzburg–Landau models for superconductivity,” in *Proceedings of the World Congress of Nonlinear Analysts 1992*, edited by V. Lakshmikantham (de Gruyter, Berlin, 1996), pp. 3789–3801.
 - ³⁴Du, Q., “Computational methods for the time dependent Ginzburg–Landau model for superconductivity,” in *Numerical Methods for Applied Sciences*, edited by W. Cai *et al.* (Science Press, New York, 1996), pp. 51–65.
 - ³⁵Du, Q., “Discrete gauge invariant approximations of a time-dependent Ginzburg–Landau model of superconductivity,” *Math. Comput.* **67**, 965–986 (1998).
 - ³⁶Du, Q., “Studies of a Ginzburg–Landau model for *d*-wave superconductors,” *SIAM J. Appl. Math.* **59**, 1225–1250 (1999).
 - ³⁷Du, Q., “Convergence analysis of a numerical method for a mean field model of superconducting vortices,” *SIAM (Soc. Ind. Appl. Math.) J. Numer. Anal.* **37**, 911–926 (2000).
 - ³⁸Du, Q., “Diverse vortex dynamics in superfluids,” *Contemp. Math.* **329**, 105–117 (2003).
 - ³⁹Du, Q., Faber, V., and Gunzburger, M., “Centroidal Voronoi tessellations: Applications and algorithms,” *SIAM Rev.* **41**, 637–676 (1999).
 - ⁴⁰Du, Q. and Gray, P., “High-kappa limit of the time dependent Ginzburg–Landau model for superconductivity,” *SIAM J. Appl. Math.* **56**, 1060–1093 (1996).
 - ⁴¹Du, Q. and Gray, P., “Numerical algorithmss of the of Lawrence-Doniach models and its parallel implementation,” *SIAM J. Sci. Comput. (USA)* **20**, 2122–2139 (1999).
 - ⁴²Du, Q., Gunzburger, M., and Ju, L., “Constrained centroidal Voronoi tessellations on general surfaces,” *SIAM J. Sci. Comput. (USA)* **24**, 1488–1506 (2003).
 - ⁴³Du, Q., Gunzburger, M., and Peterson, J., “Analysis and approximation of the Ginzburg–Landau model of superconductivity,” *SIAM Rev.* **34**, 54–81 (1992).
 - ⁴⁴Du, Q., Gunzburger, M., and Peterson, J., “Solving the Ginzburg–Landau equations by finite element methods,” *Phys. Rev. B* **46**, 9027–9034 (1992).
 - ⁴⁵Du, Q., Gunzburger, M., and Peterson, J., “Computational simulations of type-II superconductivity including pinning mechanisms,” *Phys. Rev. B* **51**, 16194–16203 (1995).
 - ⁴⁶Du, Q. and Ju, L., “Numerical simulation of the quantized vortices on a thin superconducting hollow sphere,” *J. Comput. Phys.* **201**, 511–530 (2004).

- ⁴⁷Du, Q. and Ju, L., "Approximations of a Ginzburg–Landau model for superconducting hollow spheres based on spherical centroidal Voronoi tessellations," *Math. Comput.* **74**, 1257–1280 (2005).
- ⁴⁸Du, Q., Nicolaides, R., and Wu, X., "Analysis and convergence of a covolume approximation of the G-L models of superconductivity," *SIAM (Soc. Ind. Appl. Math.) J. Numer. Anal.* **35**, 1049–1072 (1998).
- ⁴⁹Du, Q. and Remski, J., "Simplified models of superconducting normal superconducting junctions and their numerical approximations," *Eur. J. Appl. Math.* **10**, 1–25 (1999).
- ⁵⁰Du, Q. and Remski, J., "Limiting models for Josephson junctions and superconducting weak links," *J. Math. Anal. Appl.* **266**, 357–382 (2002).
- ⁵¹Du, Q. and Wu, X., "Numerical approximation of the three dimensional Ginzburg–Landau equations using artificial boundary conditions," *SIAM (Soc. Ind. Appl. Math.) J. Numer. Anal.* **36**, 1482–1506 (1999).
- ⁵²Du, Q. and Zhang, P., "Existence of weak solutions to some vortex density models," *SIAM J. Math. Anal.* **34**, 1278–1298 (2003).
- ⁵³E., W., "Dynamics of vortices in Ginzburg–Landau theories with applications to superconductivity," *Physica D* **77**, 383–404 (1994).
- ⁵⁴Elliott, C. and Styles, V., "Numerical analysis of a mean field model of superconductivity," *IMA J. Numer. Anal.* **21**, 1–51 (2001).
- ⁵⁵Enomoto, Y. and Kato, R., "Computer simulation of a two-dimensional type-II super-conductor in a magnetic field," *J. Phys.: Condens. Matter* **3**, 375–380 (1991).
- ⁵⁶Fleckinger, J., Kaper, H., and Takac, P., "Dynamics of the Ginzburg–Landau equation of superconductivity," *Nonlinear Anal. Theory, Methods Appl.* **32**, 647–665 (1998).
- ⁵⁷Frahm, H., Ullah, S., and Dorsey, A., "Flux dynamics and the growth of the superconducting phase," *Phys. Rev. Lett.* **66**, 3067–3070 (1991).
- ⁵⁸Ginzburg, V. and Landau, L., "Theory of superconductivity," *Zh. Eksp. Teor. Fiz.* **20**, 1064–1082 (1950).
- ⁵⁹Gropp, W., Kaper, H., Leaf, G., Levine, D., Plumbo, M., and Vinokur, V., "Numerical simulation of vortex dynamics in type-II superconductors," *J. Comput. Phys.* **123**, 254–266 (1996).
- ⁶⁰Gunzburger, M., Hou, L., and Ravindran, S., "Analysis and approximation of optimal control problems for a simplified Ginzburg–Landau model of superconductivity," *Numer. Math.* **77**, 243–268 (1997).
- ⁶¹Gunter, D., Kaper, H., and Leaf, G., "Implicit integration of the time-dependent Ginzburg–Landau equations of superconductivity," *SIAM J. Sci. Comput. (USA)* **23**, 1943–1958 (2002).
- ⁶²Hoffmann, K. and Zou, J., "Finite element analysis on the Lawrence-Doniach model for layered superconductors," *Numer. Funct. Anal. Optim.*, **18**, 567–589 (1997).
- ⁶³Huang, Y. and Xue, W., "Convergence of finite element approximations and multilevel linearization for Ginzburg–Landau model of d -wave superconductors," *Adv. Comput. Math.* **17**, 309–330 (2002).
- ⁶⁴Ivarsson, J., "A posteriori error analysis of a finite element method for the time-dependent Ginzburg–Landau equations," Department of Mathematics, Chalmers University of Technology (unpublished).
- ⁶⁵Jadallah, H., Rubinstein, J., and Sternberg, P., "Phase transition curves for mesoscopic superconducting samples," *Phys. Rev. Lett.* **82**, 2935–2938 (1999).
- ⁶⁶Kaper, H. and Kwong, M., "Vortex configurations in type-II superconducting films," *J. Comput. Phys.* **119**, 120–131 (1995).
- ⁶⁷Kato, M. and Sato, O., "Numerical solution of Ginzburg–Landau equation for superconducting networks," *Physica C* **392**, 396–400 (2003).
- ⁶⁸Kato, R., Enomoto, Y., and Maekawa, S., "Computer simulations of dynamics of flux lines in type-II superconductors," *Phys. Rev. B* **44**, 6916–6920 (1991).
- ⁶⁹Kogan, V., Clem, J., Deang, J., and Gunzburger, M., "Nucleation of superconductivity in finite anisotropic superconductors and the evolution of surface superconductivity toward the bulk mixed state," *Phys. Rev. B* **65**, 094514 (1-8) (2002).
- ⁷⁰Liao, H., Zhou, S., and Shi, X., "Simulating the time-dependent Ginzburg–Landau equations for type-II superconductors by finite-difference method," *Chin. Phys.* **13**, 737–745 (2004).
- ⁷¹Lin, F., "Some dynamical properties of Ginzburg–Landau vortices," *Commun. Pure Appl. Math.* **49**, 323–359 (1996).
- ⁷²Lin, F. and Du, Q., "Ginzburg–Landau vortices, dynamics, pinning and hysteresis," *SIAM J. Math. Anal.* **28**, 1265–1293 (1999).
- ⁷³Lin, F. and Lin, C., "Vortex state of d -wave superconductors in the Ginzburg–Landau energy," *SIAM J. Math. Anal.* **32**, 493–503 (2001).
- ⁷⁴Lin, F. and Zhang, P., "On the hydrodynamic limit of Ginzburg–Landau vortices," *Discrete Contin. Dyn. Syst.* **6**, 121–142 (2000).
- ⁷⁵Liu, F., Mondello M., and Goldenfeld, N., "Kinetics of the superconducting transition," *Phys. Rev. Lett.* **66**, 3071–3074 (1991).
- ⁷⁶Machida, M. and Kaburaki, H., "Direct simulation of the time-dependent Ginzburg–Landau equation for type-II superconducting thin film," *Phys. Rev. Lett.* **71**, 3206–3209 (1993).
- ⁷⁷Maurer, S., Yeh, N., and Tombrello, T., "Vortex pinning by cylindrical defects in type-II superconductors: Numerical solutions to the Ginzburg–Landau equations," *Phys. Rev. B* **54**, 15372–15379 (1996).
- ⁷⁸Moshchalkov, V., Gielen, L., Strunk, C., Jonckheere, R., Qiu, X., Van Haesendonck, C., and Bruynseraede, Y., "Effect of sample topology on the critical fields of mesoscopic superconductors," *Nature (London)* **373**, 319–321 (1995).
- ⁷⁹Mu, M., "A linearized Crank-Nicolson-Galerkin method for the Ginzburg–Landau model," *SIAM (Soc. Ind. Appl. Math.) J. Sci. Stat. Comput.* **18**, 1028–1039 (1997).
- ⁸⁰Mu, M. and Huang, Y., "An alternating Crank-Nicolson method for decoupling the Ginzburg–Landau equations," *SIAM (Soc. Ind. Appl. Math.) J. Numer. Anal.* **35**, 1740–1761 (1998).

- ⁸¹ Neu, J., "Vortices in complex scalar fields," *Physica D* **43**, 385–406 (1990).
- ⁸² Neuberger, J. and Renka, R., "Sobolev gradients and the Ginzburg–Landau functional," *SIAM (Soc. Ind. Appl. Math.) J. Sci. Stat. Comput.* **20**, 582–590 (1998).
- ⁸³ Neuberger, J. and Renka, R., "Numerical approximation of critical points of the Ginzburg–Landau functional," *Nonlinear Anal. Theory, Methods Appl.* **47**, 3259–3270 (2001).
- ⁸⁴ Neuberger, J. and Renka, R., "Computational simulation of vortex phenomena in superconductors," *J. Diff. Eqns.*, **10**, 241–250 (2003).
- ⁸⁵ X. Pan, "Surface superconductivity in applied magnetic fields above H_{c2} ," *Commun. Math. Phys.* **228**, 327–370 (2002).
- ⁸⁶ Ren, Y., Xu, J., and Ting, C., "Ginzburg–Landau equations and vortex structure of a $d_{x^2-y^2}$ superconductor," *Phys. Rev. Lett.* **74**, 3680–3683 (1995).
- ⁸⁷ Rubinstein, J. and Sternberg, P., "On the slow motion of vortices in the Ginzburg–Landau heat flow," *SIAM J. Math. Anal.* **26**, 1452–1466 (1995).
- ⁸⁸ Sandier, E. and Serfaty, S., "On the energy of type-II superconductors in the mixed phase," *Rev. Math. Phys.* **12**, 1219–1257 (2000).
- ⁸⁹ Schweigert, V., Peeters, F., and Deo, P., "Vortex phase diagram for mesoscopic superconducting disks," *Phys. Rev. Lett.* **81**, 2783–2786 (1998).
- ⁹⁰ Tang, Q. and Wang, S., "Time dependent Ginzburg–Landau superconductivity equations," *Physica D* **88**, 139–166 (1995).
- ⁹¹ Tinkham, M., *Introduction to Superconductivity*, 2nd ed. (McGraw-Hill, New York, 1994).
- ⁹² Wang, Z. and Hu, C., "A numerical relaxation approach for solving the general Ginzburg–Landau equations for type-II superconductors," *Phys. Rev. B* **44**, 11918–11923 (1991).
- ⁹³ Wang, Z. and Wang, Q., "Vortex state and dynamics of a d -wave superconductor: Finite-element analysis," *Phys. Rev. B* **55**, 11756–11765 (1997).
- ⁹⁴ Winiecki, T. and Adams, C., "A fast semi-implicit finite difference method for the TDGL equations," *J. Comput. Phys.* **179**, 127–139 (2002).
- ⁹⁵ Zhan, M., "Finite element analysis and approximations of phase-lock equations of superconductivity," *Discrete Contin. Dyn. Syst., Ser. B* **2**, 95–108 (2002).